



HAL
open science

Excited state absorption: a key phenomenon for the improvement of biphotonic based optical limiting at telecommunication wavelengths

Quentin Bellier, Nikolay S. Makarov, Pierre-Antoine Bouit, Stéphane Rigaut, Kenji Kamada, Patrick Feneyrou, Gérard Berginc, Olivier Maury, Joseph W. Perry, Chantal Andraud

► To cite this version:

Quentin Bellier, Nikolay S. Makarov, Pierre-Antoine Bouit, Stéphane Rigaut, Kenji Kamada, et al.. Excited state absorption: a key phenomenon for the improvement of biphotonic based optical limiting at telecommunication wavelengths. *Physical Chemistry Chemical Physics*, 2012, 14 (44), pp.15299-15307. 10.1039/C2CP40779E . hal-00833259

HAL Id: hal-00833259

<https://hal.science/hal-00833259>

Submitted on 26 Nov 2019

HAL is a multi-disciplinary open access archive for the deposit and dissemination of scientific research documents, whether they are published or not. The documents may come from teaching and research institutions in France or abroad, or from public or private research centers.

L'archive ouverte pluridisciplinaire **HAL**, est destinée au dépôt et à la diffusion de documents scientifiques de niveau recherche, publiés ou non, émanant des établissements d'enseignement et de recherche français ou étrangers, des laboratoires publics ou privés.

**Excited state absorption: a key phenomenon for the improvement of
biphotonic based optical limiting at telecommunication wavelengths.**

Quentin Bellier,^a Nikolay S. Makarov,^b Pierre-Antoine Bouit,^a Stéphane Rigaut,^c Kenji Kamada,^d Patrick FeneYROU,^e Gérard Berginc,^e Olivier Maury*^a, Joseph W. Perry*^b, and Chantal Andraud*^a.

- a. *Ecole Normale Supérieure de Lyon, CNRS-UMR 5182, Université de Lyon 1, 46 Allée d'Italie, F-69364 Lyon cedex 07, France, chantal.andraud@ens-lyon.fr.*
- b. *School of Chemistry and Biochemistry, Center of Organic Photonics and Electronics, Georgia Institute of Technology, 901 Atlantic Drive, NW Atlanta, GA 30332-0400, USA, joe.perry@chemistry.gatech.edu.*
- c. *Sciences Chimiques de Rennes, UMR 6226 CNRS-Université de Rennes 1, Campus de Beaulieu, 35042 Rennes cedex, France.*
- d. *Research Institute for Ubiquitous Energy Devices, National Institute of Advanced Industrial Science and Technology (AIST), AIST Kansai Center, 1-8-31 Midorigaoka, Ikeda, Osaka 563-8577, Japan.*
- e. *Thales Research & Technology France, Route Départementale 128, 91767 Palaiseau Cedex, France.*

Abstract

Spectroscopic properties, two-photon absorption (TPA) and excited state absorption (ESA), of two organic cyanine dyes and of a ruthenium based organometallic cyanine are compared in order to rationalize their similar ns-optical power limiting (OPL) efficiency in telecommunication wavelength range. The TPA contribution to the ns-OPL behavior is higher for both organic cyanines, while the main process is a TPA-induced ESA in the case of the organometallic system, in which the ruthenium induces a broadening of the NIR-ESA band and then a strong spectral overlap between TPA and ESA spectra.

Introduction

Optical power limiters (OPL) are devices that are able to protect detectors (eyes, sensors...) against intrusive laser beams by limiting the transmitted intensity below the material damage threshold, while remaining transparent under low power irradiation.¹ Such devices have already been widely developed to address visible (400-1000 nm) laser sources. OPL functionality can be obtained by taking advantage of a large variety of physical phenomena like multiphoton absorption,² reverse saturable absorption,³ nonlinear refraction or nonlinear scattering.⁴ In this context, nonlinear optical (NLO) materials with strong two-photon absorption (TPA) properties have attracted a great deal of attention since the material response is extremely fast because it is triggered by the incident light itself. The requirements for the design of such molecular optical limiting materials include the following properties: (i) high two-photon absorption cross-section ($\sigma^{(2)} \sim 1000 \text{ GM}$; $1 \text{ GM} = 10^{-50} \text{ cm}^4 \cdot \text{s} \cdot \text{photon}^{-1} \cdot \text{molecule}^{-1}$), (ii) high solubility in organic solvent or in a host matrix, and (iii) good photostability under laser irradiation. In addition, it has been demonstrated that a good spectral overlap between excited state absorption (ESA, characterized by the excited state cross-section, $\sigma^{(\text{ESA})}$) and TPA

at the incident laser wavelength can dramatically enhance the OPL properties. Indeed during the laser pulse duration, the following photophysical processes can occur: TPA, a nonlinear phenomenon that promotes a molecule to an excited state followed by ESA, a linear optical process that strongly enhances the overall absorption efficiency of the whole process (Fig. 1). Whereas molecular engineering rules for TPA optimization are quite well established,⁵ far less is known about optimization of ESA. However, it is generally recognized that increasing the excited state lifetime enhances ESA probability,⁶ and this consideration has triggered the development of chromophores in which the inter-system crossing (ISC) is favorable, resulting in the population of a long-lived triplet excited state (T_1) (Fig. 1). To that end, chromophores featuring heavy atoms like bromine, platinum, and ruthenium, for example, are known to facilitate ISC process, and have been successfully designed to enhance OPL applications in the visible spectral range.⁷

Over the past decade, laser sources in the near infrared spectral range (NIR, 1100 -1660 nm) have become widely used in optical telecommunications and laser range finders, which has stimulated the design of new chromophores for NIR-OPL applications, as well as telecommunication devices, based on two-photon absorption. Since 2005, numerous dyes, *e.g.* dipolar or quadrupolar polyenes, π -conjugated oligomers, singlet diradical molecules, cyanine, squaraine, poly(porphyrins), bodipy, among others have been developed,⁸ and very large TPA cross-sections have been achieved. It is worth noting that among all these chromophores developed for NIR-TPA applications, only four examples of NIR-OPL have been realized, and these were based on heptamethine cyanine (**1**),⁹ functionalized (aza)-bodipy^{10, 11} or bis(ethynyl)-lead porphyrine oligomer¹² (Fig. 1).

In this article, we describe the TPA, ESA and OPL properties in the NIR spectral range of three chromophores belonging to the general family of “cyanine dyes” (Fig. 2) and we illustrate the influence of the ruthenium atoms in the terminal positions of the conjugated

cyanine skeleton on physical properties of the molecule. We show that, in spite of the presence of Ruthenium atoms, singlet-singlet transitions are involved in the ESA dynamics, and, as already observed in visible, we confirmed that the spectral overlap between NIR-ESA and NIR-TPA properties is a key requirement to enhance the optical limiting behavior at telecommunication wavelengths.

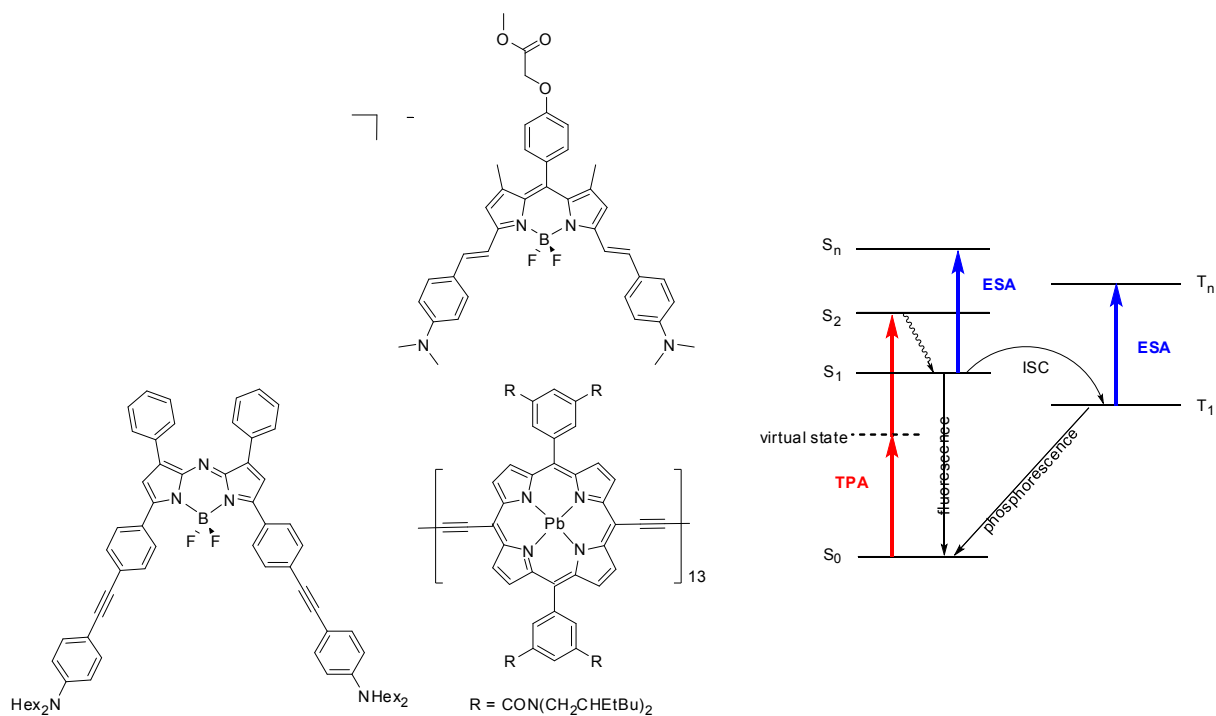


Figure 1. Chromophores successfully involved in NIR-OPL applications.

Results

Chromophores. Figure 2 depicts the structure of the three chromophores examined in this study. **1** is an archetype of cyanine dyes, and more precisely an heptamethine cyanine since the cationic charge is delocalized over seven carbon atoms. The cyclohexenyl moieties combined with the *tert*-Bu functionality impart good stability and solubility as required to carry out optical limiting measurements. **2** is one of the rare oxonol-type derivatives reported in the literature with a negative charge delocalized between two strong acceptors.¹³ These two compounds exhibit zero bond-length alternation (BLA) according to their X-ray diffraction structures and theoretical geometry optimization (DFT) and present absorption transitions at 794 and 900 nm, respectively, with giant extinction coefficients and typical cyanine bandshapes (Table 1 and Fig. 3).^{13, 14} These two compounds are also emissive in the NIR spectral range (Fig. 4) with a sharp emissions centered at 823 and 939 nm, respectively, and mono-exponential luminescence decays ($\tau(\mathbf{1}) = 1.18$ ns, $\tau(\mathbf{2}) = 0.39$ ns). On the other hand, the bimetallic complex **3** displays a cationic charge fully delocalized between two electro-donating ClRu(dppe)₂-moieties (dppe = 1,2-bis(diphenylphosphino)ethane) over a seven carbon atoms conjugated chain (Fig. 2). The simple BLA parameter cannot be calculated due to the presence of the triple bond but the ground-state structure is fully delocalized as illustrated by solution NMR data, X-ray diffraction structure and DFT calculation¹⁵ with bond lengths intermediate between (i) single and double bond for the W-shaped bridge and (ii) ruthenium allenylidene and ruthenium acetylide moieties for the [Ru-C-C-C] linear fragments. A similarly high degree of delocalization and large third-order optical nonlinearity has been reported for a bis-porphyrin pentadiyne cation.¹⁶ In addition, the Ru complex exhibits an intense broad absorption at 764 nm but no emission in dichloromethane ($c \sim 10^{-6}$ M, optical density < 0.1) and can therefore be considered as an organometallic cyanine (Fig. 3 and Table 1).

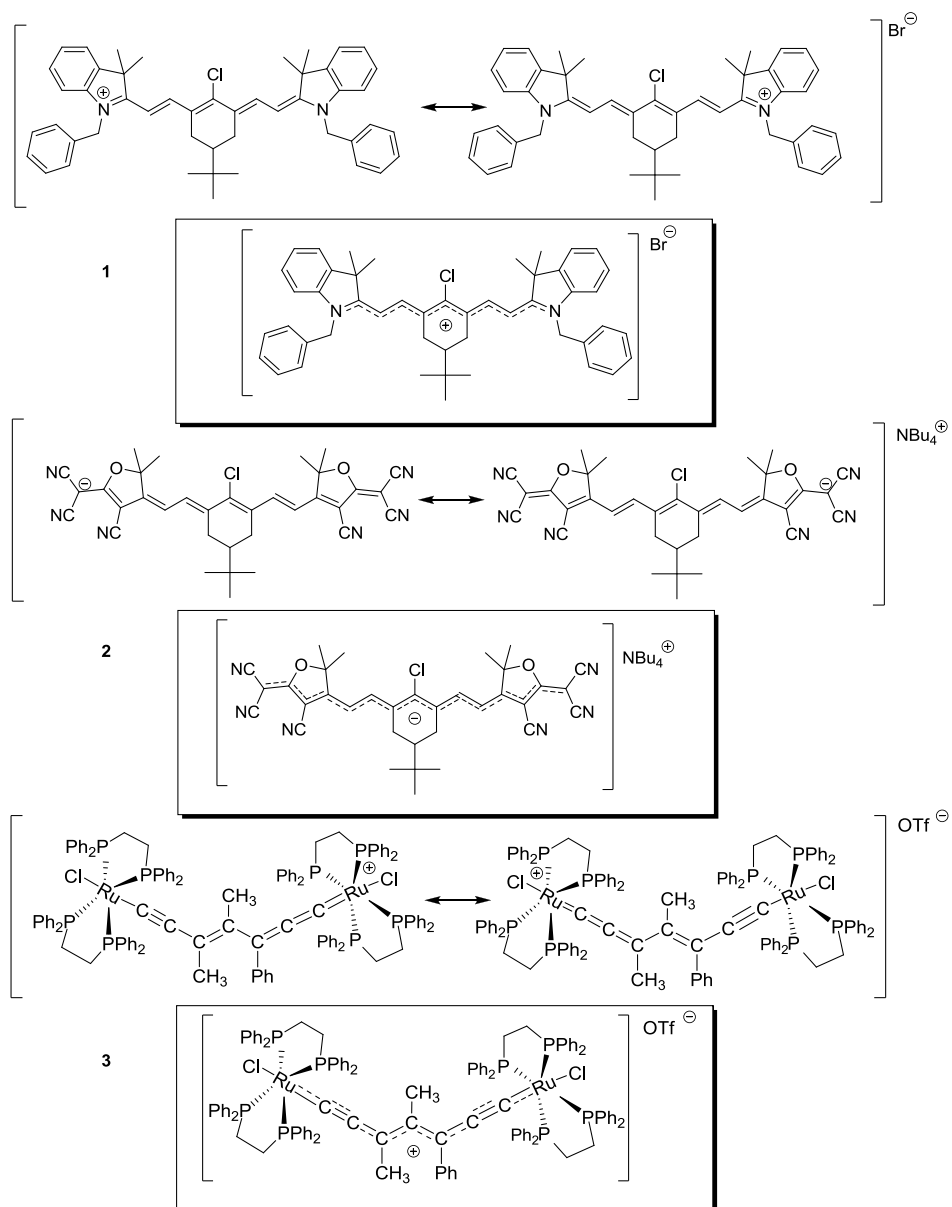


Figure 2. Structure of the cyanine type chromophores.

Table 1. Photophysical data in dichloromethane of **1-3**.

| compound | λ_{\max} (nm) | ε (L.mol ⁻¹ cm. ⁻¹) | $\lambda_{\max}^{(2)}$ (nm) | $\sigma^{(2)}$ (GM) | $\lambda_{\max}^{(\text{ESA})}$ (nm) | $\sigma^{(\text{ESA})}$ (cm ²) |
|----------|--------------------------|---|--------------------------------|------------------------|---|---|
| 1 | 794 | 290000 | 1437 | 731 | 1290 | 9.9×10^{-17} |
| 2 | 900 | 325000 | 1592 | 890 | 1255 | 0.5×10^{-17} |
| 3 | 764 | 109000 | 1408 | 133 | 1515 | 9.8×10^{-17} |

Two-photon absorption. NIR-TPA measurements were carried out in concentrated dichloromethane solution using the open-aperture Z-scan method in the 1200-1800 nm spectral range. The incident light source consists of a fs-optical parametric amplifier pumped by Ti:sapphire source (1kHz, 130 fs pulse).¹⁷ At such short pulse duration, pure TPA is generally considered and the propagation equation (1) can be simplified to read:

$$dI/dz = -\alpha^{(2)}I^2 \quad (1)$$

where I represents the laser intensity, z is the propagation direction, and $\alpha^{(2)}$ is the two-photon absorption coefficient. The molecular two-photon cross-section can then be simply deduced according to the relationship (2):

$$\sigma^{(2)} = h\nu\alpha^{(2)}/N \quad (2)$$

where N represents the number density of molecules in the solution and $h\nu$ is the photon energy at the operating wavelength. Typical open-aperture Z-scan traces (normalized transmittance scaled to that at a sample position enough away from the focal point to ignore the nonlinear absorption, versus the sample position z) obtained are shown in Fig. 4A. A clear dip centered at the focal position ($z = 0$), indicating nonlinear absorption, was observed and evolved as increasing the incident laser power. For other wavelengths and other samples, the similar Z-scan traces were obtained (see Electronic Supplementary Information). From the curve fit to each observed z-scan trace, two-photon absorbance q_0 was obtained. The plot of q_0 against the average incident power (thus, against the optical intensity of the incident pulse) shows a proportional relation (Fig. 4B), confirming dominant contribution of the observed nonlinear signal originates from TPA. The slope of this plot gives $\alpha^{(2)}$ of the sample and the TPA cross section $\sigma^{(2)}$ was calculated with eq. 2. Typical experimental error for $\sigma^{(2)}$ was $\pm 15\%$ or less. More details of the analysis are shown in Experimental section. Scanning the wavelength and repeating the measurements at each wavelength, TPA spectrum of the compounds **1–3** were obtained (Fig. 5).

As already observed for other cyanine dyes, the TPA spectra of **1** and **2** are blue-shifted compared to the wavelength-doubled one-photon absorption (OPA) as shown in Fig. 5.^{9a} The TPA peaks, however, correspond to the position of the sideband in the OPA spectra generally assigned to a vibronic contribution, suggesting that Herzberg-Teller-type vibronic coupling via an anti-symmetric B_1 vibrational mode of the conjugated chain is, likely responsible for the strength of the TPA band.¹⁸

As expected, the anionic cyanine **2**, which exhibits the most red-shifted OPA spectrum, presents also a TPA spectrum at lower energy with respect to **1** with a TPA maximum wavelength at 1600 nm and a TPA cross-section up to 800 GM (Fig. 5 and Table 1). TPA cross-sections for **1**

and **2** are relatively large compared to aza-based cyanine dyes,¹⁹ which generally have values between ~ 100 and 250 GM, but in the same range as those of aza-bodipy,¹⁰ dipolar or quadrupolar chromophores²⁰ and far lower than that of extended conjugated squaraine and self-assembled or fused porphyrins.²¹ In marked contrast with **1** and **2**, the organometallic cyanine **3** exhibits weak TPA properties with a rather low cross-section (< 150 GM) over the 1350 - 1550 nm spectral range.

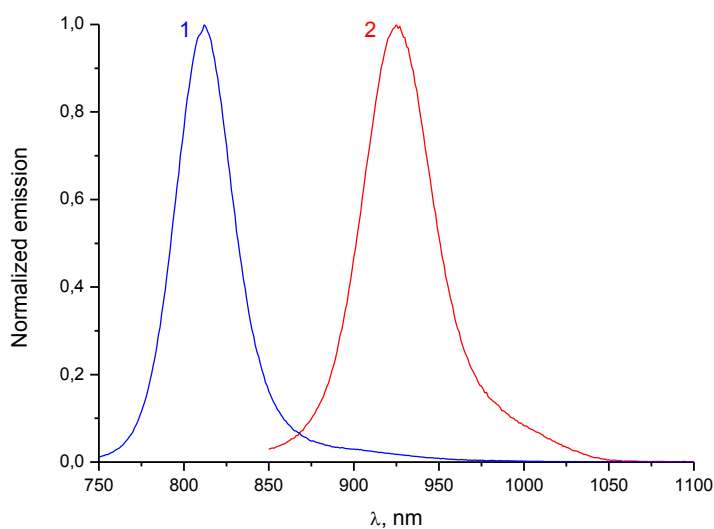


Figure 3. Emission spectra in dichloromethane solution of **1** (blue), **2** (red). Dye **3** does not present any emission in this solvent.

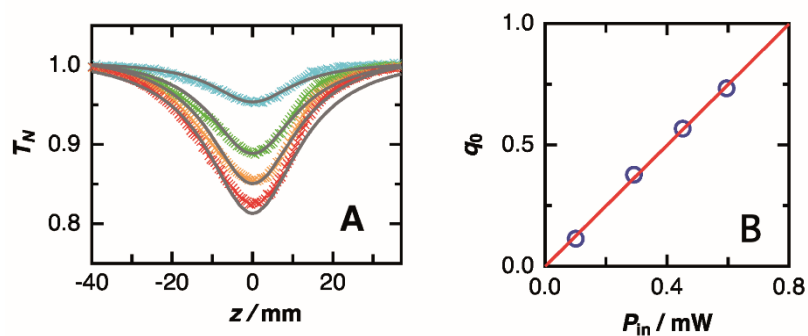


Figure 4. (A) Open-aperture Z-scan traces (normalized transmittance T_N versus sample position z) of **2** in dichloromethane ($4.5 \text{ mmol}\cdot\text{L}^{-1}$) at 1600 nm with various incident powers ($P_{\text{in}} = 0.10, 0.29, 0.45,$ and 0.59 mW , from the top to bottom). The data point are shown in cross together with the theoretical fitting curve (see the text) in solid line. (B) Plot of two-photon absorbance q_0 obtained from the curve fitting from the data in panel A versus P_{in} .

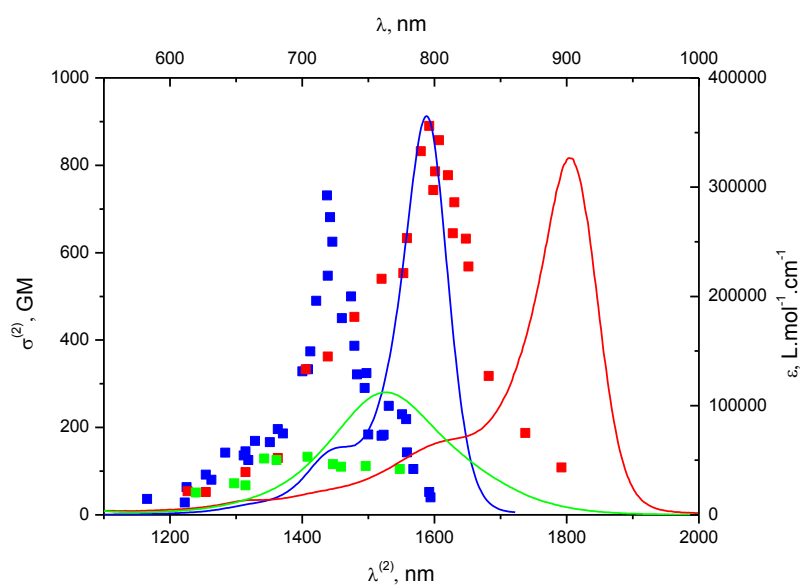


Figure 5. Absorption (lines) and two-photon absorption (squares) spectra in dichloromethane for **1** (blue), **2** (red) and **3** (green).

Excited state absorption. As it has been widely established that TPA based optical power limiting properties can be rationalized in terms of three-photon absorption involving ESA, transient absorption properties of molecules **1-3** have been studied. Figure 6 shows the transient absorption spectra obtained for compounds **1-3** at a small time delay ($\sim 5 \text{ ps}$) between the pump and the probe beams. The spectra show reasonably strong excited state transitions at short probe wavelengths, $\sim 547 \text{ nm}$ for **1**, $\sim 587 \text{ nm}$ for **2**, and $\sim 755 \text{ nm}$ for **3**, which is typical

for cyanine molecules, and usually corresponds to the transition from lowest one-photon excited state to a higher excited state. At longer probe wavelengths, there is evidence of the transient bleaching of the OPA band which is strongly dominated by a peak due to stimulated emission. The molecule **3** also shows some bleaching in its second OPA band, at ~520 nm. At the wavelengths higher than 1000 nm, all three compounds show an ESA peak (intermediate strength at ~1290 nm for **1**, low strength at ~1255 nm for **2**, and broad with intermediate strength at ~1520 nm for **3**). This band is typically attributed to a quasi-OPA-forbidden state. All the ESA peaks of **1** and **2** show monoexponential decays with the lifetimes of ~1090 ps and ~385 ps, respectively, which is consistent with the luminescence decay data. All the peaks of **3** are characterized by a bi-exponential decay with the lifetimes of ~220 ps and ~1480 ps. All lifetimes suggest that even for the heavy-atom molecule **3**, only the singlet-singlet transitions are involved in the ESA dynamics.

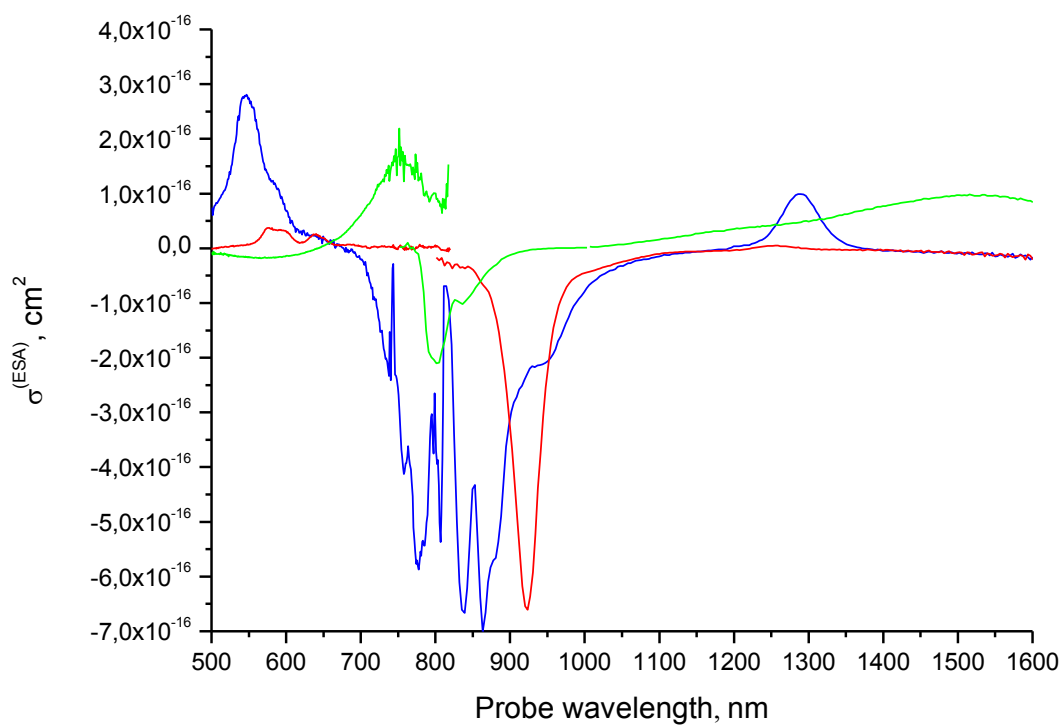


Figure 6. Excited state absorption spectra of **1** (blue), **2** (red) and **3** (green) in dichloromethane solution.

Optical limiting. The optical limiting properties of dyes **1-3** were determined in solution over the 1300-1600 nm spectral range every ca. 50 nm in a 2 mm quartz cell using focused pulses from an optical parametric oscillator (pulse duration 7 ns, 10 Hz) laser source. The high solubility and large scale availability of compounds **1-3** allows to prepare the sample as a highly concentrated (about $0.1 \text{ mol}\cdot\text{L}^{-1}$) dichloromethane solution. For each sample, the variation of the transmittance vs. incident laser fluence at the telecommunication wavelength of 1500 nm is represented in Figure 7; similar curves were obtained over the entire spectral range of 1300-1600 nm. In all cases, the characteristic response of an optical limiter is observed, *i.e.* a good linear transmission (> 0.9) at low energy and nonlinear attenuation when the laser fluence is over a threshold of between $0.4\text{-}0.8 \text{ J cm}^{-2}$ depending on the molecule. The maximal drop of the transmission was 40% for the highest laser fluence allowed by our experiment set-up (2 J cm^{-2}).

The ns-OPL experimental curves were first analyzed on the basis of equation (1) involving a pure TPA process. The $\sigma^{(2)}$ value is calculated according to equation (2), using the concentration and the $\alpha^{(2)}$ coefficient measured by fs-Z-scan. The theoretical simulations represented in blue in Figure 6 exhibit a very large deviation from the experimental data, indicating that the model based on a pure TPA process is insufficient to describe the response. Such a difference has been observed previously, when the pulse duration of the OPL experiment is in the same order of magnitude (even longer) than the lifetime of the molecular excited states. This is clearly the case here since the pulse duration is about 7 ns, and the lifetime of the cyanine excited state measured by fluorescence decay is estimated to 1.18 ns and 0.39 ns for **1** and **2**

respectively. As a consequence, a high-order optical absorption phenomena must be taken into account such as TPA-induced ESA, for which the propagation equation becomes:

$$dI/dz = -\alpha^{(2)}I^2 - \alpha^{(3)}I^3 \quad (3)$$

assuming a negligible OPA in the spectral range of interest ($\alpha^{(1)} = 0$) and with $\alpha^{(3)}$ being the effective three-photon absorption coefficient representing the TPA-induced ESA process. The value of $\alpha^{(3)}$ was determined by a numerical solution of the propagation equation according a procedure previously described⁹: The two-photon absorption coefficient is numerically set to the corresponding value measured using fs Zscan and the TPA-induced ESA coefficient $\alpha^{(3)}$ is adjusted so that the computed nonlinear transmission corresponds to the measured value on the ns-OPL setup. The nonlinear transmission is computed assuming a Gaussian profile for both time dependency and transverse beam shape. The pulse duration is measured independently using fast response photodiode and the beam shape is also measured independently using InGaAs camera so that the equation (3) can be integrated with a single unknown : the TPA-induced ESA coefficient $\alpha^{(3)}$. The simulations (green lines in the Fig. 7) fit well with the experiment data. This result clearly indicates that, for all studied compounds, the ns-OPL response involve a TPA-induced ESA photophysical process.

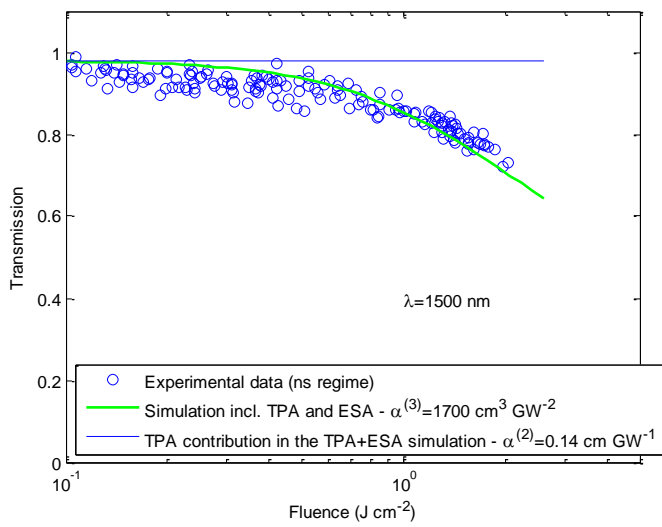
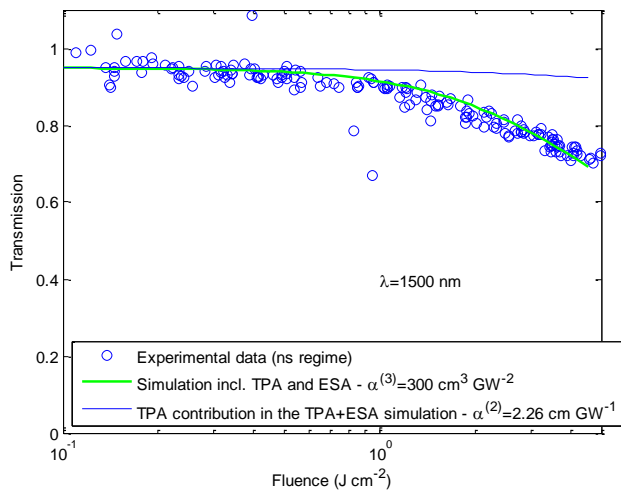
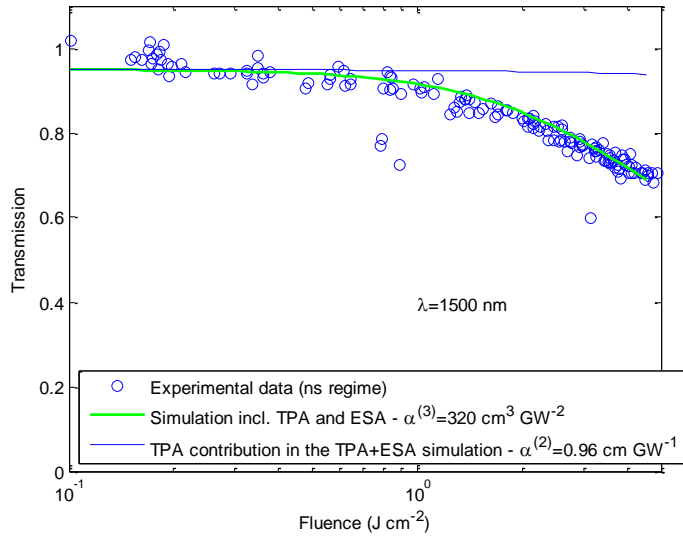
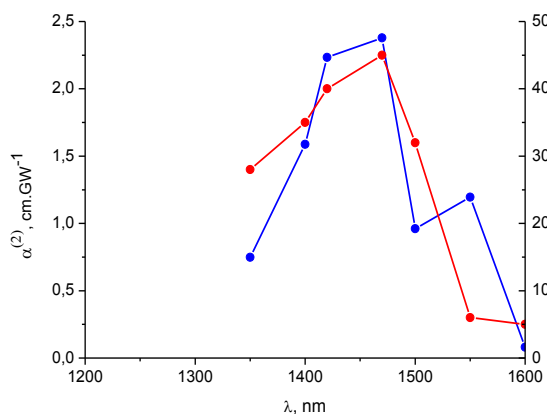


Figure 7. Optical limiting in concentrated dichloromethane solution at 1500 nm for compounds **1** (up), **2** (middle) and **3** (bottom). Experimental data points are represented by blue circles, theoretical simulations using a simple model including only the TPA contribution are displayed in blue lines, while the fit using a model including TPA-induced ESA are depicted in green line.

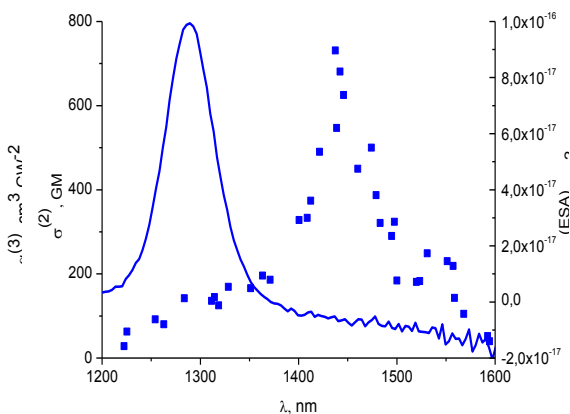
Discussion

For all compounds examined, the NIR-OPL experiments have been performed at the same concentration (0.1 mol L⁻¹). Therefore, it is possible to compare the concentration dependent $\alpha^{(2)}$ and $\alpha^{(3)}$ coefficients. On one hand, the $\alpha^{(2)}$ coefficients were obtained from fs-Z-scan experiments and Equation (2). On the other hand, the ns-OPL experiments have been performed at different wavelengths between 1300 and 1600 nm and the spectral variations of the $\alpha^{(3)}$ coefficient were determined by fitting the OPL response to the combined two- and three photon absorption model, Equation (3). The results are presented in the left part of the Figure 7. One can notice that the three compounds present roughly the same OPL efficiency with peak $\alpha^{(3)}$ coefficients, between 400 and 2000 cm³·GW⁻², at telecommunication wavelengths. However, a major difference in behavior among the three compounds **1-3** should be highlighted: the $\alpha^{(2)}$ coefficients of both organic cyanine dyes **1** and **2** are about 2.5-4.0 cm·GW⁻¹, one order of magnitude higher than that of **3** (0.2 cm·GW⁻¹). This indicates that, especially for molecule **3**, an additional phenomenon other than TPA must be included to describe its OPL response. The comparison between TPA and ESA spectra allows us to make the following conclusions on the origin of OPL efficiency for molecules **1-3**: (i) for **1** and **2**, the TPA and ESA bands are quite sharp and the large difference between $\lambda_{\max}^{(2)}$ and $\lambda_{\max}^{(\text{ESA})}$ (Table 1) results in a small spectral overlap between TPA and ESA (right part in Fig. 8). This observation and the simulations of the OPL response indicate that the TPA phenomenon makes a larger contribution to the OPL

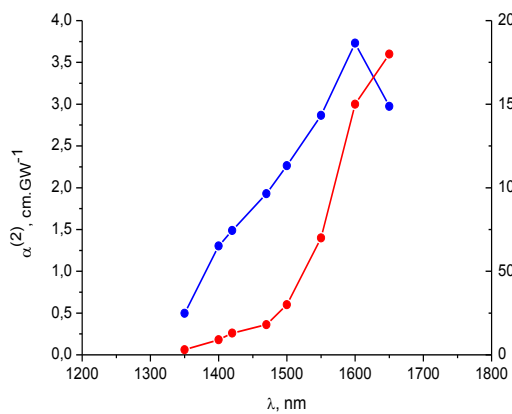
efficiency of both **1** and **2** as compared to **3**. (ii) On the contrary, in the case of **3**, the TPA and ESA bands are broader and both exhibit excellent spectral overlap over the 1300-1500 nm range. Consequently, in spite of a lower TPA efficiency, the compound **3** exhibits a similar OPL efficiency to the organic cyanines **1** and **2** due to the favorable spectral overlap of TPA and ESA.



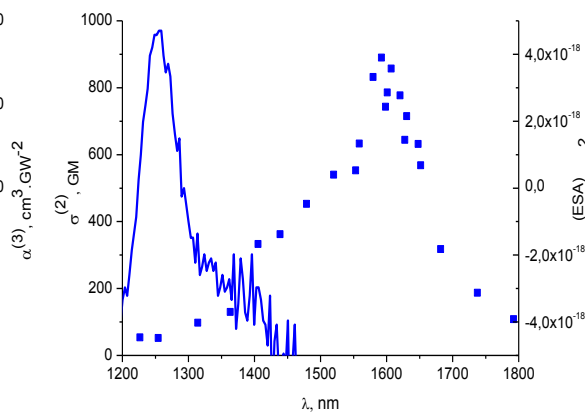
a-1



a-2



b-1



b-2

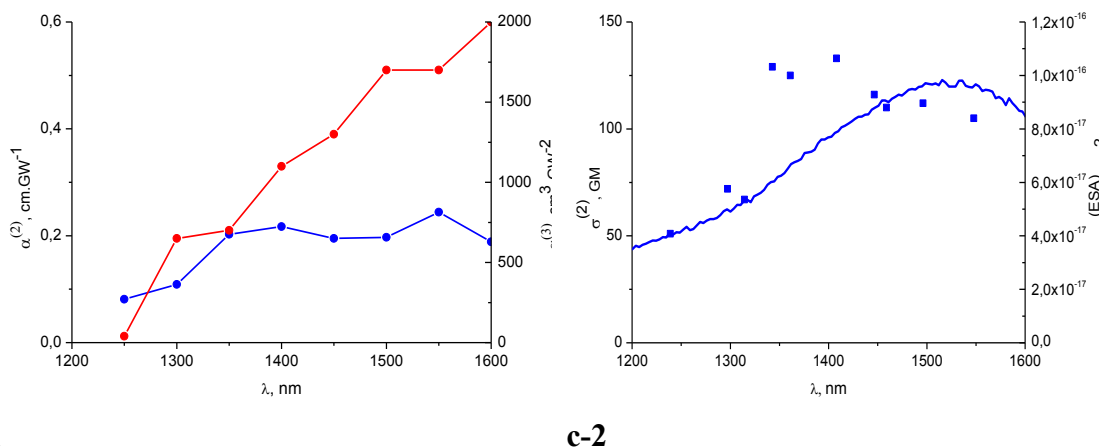


Figure 8. (left) Spectral variations of $\alpha^{(3)}$ (red curve) deduced from ns-OPL experiments and $\alpha^{(2)}$ (blue curve) deduced from fs Z-scan experiments in the case of **1** (a-1), **2** (b-1) and **3** (c-1). (right) Comparison between NIR-TPA (blue squares) and NIR-ESA (blue solid line) spectral variations in the case of **1** (a-2), **2** (b-2) and **3** (c-2).

Conclusion.

We have present a detailed photophysical study of two organic cyanine dyes and a ruthenium based organometallic cyanine. For each compound, the two-photon absorption and excited stated absorption spectra were measured in the NIR range. The three compounds exhibit optical limiting behavior for nanosecond pulses in the telecommunication wavelength range with a similar efficiency. Whereas the TPA contribution to the ns-OPL behavior is stronger in the case of organic cyanines **1** and **2**, the TPA-induced ESA is the predominant photophysical process in the case of the organometallic cyanine **3**. This difference is due to a strong spectral overlap between TPA and ESA spectra for **3**. It highlights that the role of the ruthenium atoms is mainly to induce a broadening of the NIR-ESA band, resulting in optimal spectral overlap between ESA and TPA and consequently a good OPL efficiency.

Experimental.

Absorption and emission. Absorption spectra were recorded on a JASCO V-650 spectrophotometer in dilute dichloromethane solution. Emission spectra were measured using a Horiba-Jobin-Yvon Fluorolog-3 iHR320 fluorimeter. The steady-state luminescence was excited by unpolarized light from a 450W xenon CW lamp and detected at an angle of 90° for diluted solution measurements (10 mm quartz cuvette) by a red-sensitive water-cooled Hamamatsu R2658P photomultiplier tube. Spectra were corrected for both the excitation source light intensity variation and the emission spectral response. The luminescence decay were monitored using TC-SPC Horiba apparatus using Ludox in distilled water to determine the instrumental response function used for deconvolution. Excitation was performed using Nanoled-740 (peak wavelength 732 nm, duration 1.3 ns) and the deconvolution was performed using the DAS6 fluorescence-decay analysis software.

Transient absorption. Excited state absorption spectra were measured using Ultrafast Systems Helios nonlinear spectrometer as was described earlier.¹¹ The measurements were done in a 2-mm long quartz cuvette with the peak optical densities of the samples ~0.8-1.2. An output of an 1-KHz rep. rate Ti:Sapphire regenerative amplifier (Spitfire, Spectra-Physics) was split between the seed for white-light supercontinuum probe beam, and a pump for optical parametric amplifier (TOPAS-C, Light-Conversion) whose output was used to pump samples into excited state with the incident pump pulse energy on the sample ~0.27-0.33 μJ . All the spectra were collected by exciting samples at their lowest energy bands. The excited state cross sections were estimated based on numerical beam propagation code.¹¹

Z-Scan Set-up. Two-photon absorption spectra were measured by using an open aperture Z-scan method between 1200 and 1600 nm with a fs-optical parametric amplifier (OPA-800,

Spectra-Physics) pumped by a Ti:sapphire regenerative amplifier laser operating at 1 kHz as a light source. Typical pulse duration was 130 fs. Details of the setup were published previously.¹⁷ The pulsewidth t_p on each set of the measurements at a wavelength selected was evaluated by the autocorrelation ($t_p = 120\text{--}140$ fs in FWHM) and used for the analysis of each trace. The autocorrelation profiles were reasonably fitted with by a Gaussian function, thus we assume Gaussian temporal profile for the analysis. For the spatial profile, the output laser beam from the optical parametric amplifier was expanded through a telescope and then the central part of the expanded beam was allowed to pass a small circular aperture. The transmitting beam through the aperture (ca. 10% of the total input power) was led to the Z-scan optics. This procedure gives a quasi-Gaussian spatial profile, know as Airy pattern, at the focal point of the measurement setup. Although the z -dependence of the optical intensity of this beam by Fraunhofer diffraction is not exactly the same as that of ideal Gaussian beam, numerical simulations under our standard experimental condition show that the curve fits with the assumption of Gaussian beam shown below to a simulated z -scan trace by Fraunhofer diffraction beam and to that by Gaussian beam gives virtually identical results with a deviation less than a few percents, which is less than the experimental errors typically $\pm 15\%$, When a temporally- and spatially-Gaussian pulse propagates through a TPA media, the energy transmittance is obtained as a function of the sample position:¹⁷

$$T(\zeta) = T_i \frac{1}{\sqrt{\pi q(\zeta)}} \int_{-\infty}^{\infty} \ln[1 + q(\zeta)e^{-x^2}] dx \quad (4)$$

With:

$$q(\zeta) = \frac{q_0}{1 + \zeta^2} \quad (5)$$

where ζ is the normalized sample position defined as $\zeta = z/z_R$ (z_R is the Rayleigh range). $T(\zeta)$ is the normalized transmittance as a function of ζ . The term of is liner transmittance by the one-photon absorption, where $\alpha^{(1)}$ is the one-photon absorption coefficient, L is the physical length of the sample, and R is the Fresnel reflectance at the cell surface. q_0 is the two-photon absorbance, as analogue of absorbance in one-photon absorption, at the focal position ($\zeta = 0$) defined as:

$$q_0 = \alpha^{(2)} I_0 (1-R) L_{\text{eff}} \quad (6)$$

where $\alpha^{(2)}$ is TPA coefficient, I_0 is the on-axis peak intensity of the temporally- and spatially-Gaussian pulse, and L_{eff} is the effective path length defined as $L_{\text{eff}} = [1 - \exp(-\alpha^{(1)}L)]/\alpha^{(1)}$. In the present case, the one-photon absorption at the wavelengths employed is negligible for all samples and thus L_{eff} is reduced to L . A plot of q_0 against the average incident power (thus, against I_0) shows a proportional relation (Fig. 4B) as expected from eq. 2, exhibiting the observed nonlinear signal originate from TPA. The slope of the plot gives $\alpha^{(2)}$ of the sample. At each wavelength, the open-aperture traces were recorded by changing the average incident power of the laser beam from 0.1 to 0.7 mW corresponding to the on-axis peak intensity at the focal point I_0 of 7~80 GW cm⁻² depending on the Rayleigh range ($z_R = 11\sim 14$ mm) as shown in Fig. 4. The sample solutions in spectroscopic grade dichloromethane (2–5 mmol·L⁻¹) poured in a 1-mm quartz cuvette were used for the measurements. The longer z_R than the length of the sample ($L = 1$ mm) fulfills the optically-thin condition with which eq. 4 is valid²².

Optical limiting set-up. The nonlinear transmittance measurements (transmission versus incident energy) were performed with a wavelength tunable laser source: a third-harmonic of a Q-switched Nd:YAG laser pumping an optical parametric oscillator delivering 7 ns-long pulses. The laser beam was spatially filtered, and then focused onto the dye solution. Reference energy

was taken using a coated wedged flat. The transmitted energy was focused on the signal detector. Typical beam waist $\omega_0 \approx 60 \mu\text{m}$ ($\text{HW1/e}^2\text{M}$) was measured at each test wavelength by imaging the focal plane on a InGaAs camera. The position of dye sample was adjusted at each wavelength so that its transmission under high flux is minimum (open aperture Z-scan). The incident energy was then controlled by combination of an achromatic half-wave plate and a polarizer. Incident energy was measured using a calibrated Germanium probe (Laser Precision RJP-495) and transmitted energy was measured using pyro-electric probe (Laser Precision RJP-735). Typical beam waist was chosen in order to get high incident energy densities in the sample while achieving a Rayleigh range higher than the 2 mm thickness of the cells. The beam characteristics and the experimental setup were chosen to minimize the influence of defocusing effects:

- the pulse repetition rate (10Hz) is much smaller than the reciprocal thermal diffusion time in the cell ($\tau_d = \omega_0^2/D \sim 4 \mu\text{s}$).
- the solvent (dichloromethane) and the beam waist are chosen in order to get a long acoustic transient time ($\tau_{ac} = \omega_0/C_s = 60 \text{ ns}$ where C_s is the speed of sound) : the pulse width is small compared to the acoustic transient time. Therefore, the sensitivity of the measurement to nonlinear refraction is reduced.²³
- the collecting lens aperture (which is twice the size of the beam in linear regime) and the detector size were chosen so that all the transmitted light is collected and focused onto the detector even under high incident flux.

With these experimental precautions, no aperture losses due to defocusing effects were observed.

References and Notes.

-
- 1 W. C. Spangler, *J. Mater. Chem.* 1999, **9**, 2013-2020.
- 2 a) J. E. Ehrlich, X. L. Wu, I. Y. S. Lee, Z. Y. Hu, H. Röckel, S. R. Marder, J. W. Perry, *Opt. Lett.* 1997, **22**, 1843-1845; b) Y. Morel, A. Irimia, P. Najechalski, Y. Kervella, O. Stephan, P. L. Baldeck, C. Andraud, *J. Chem. Phys.* 2001, **114**, 5391-5396; c) G. S. He, J. D. Bhawalkar, P. N. Prasad, B. A. Reinhardt, *Opt. Lett.* 1995, **20**, 1524-1526; d) J. D. Bhawalkar, G. S. He, P. N. Prasad, *Optics Comm.* 1995, **119**, 587-590.
- 3 a) D. Dini, M. Barthel, M. Hanack, *Eur. J. Org. Chem.* 2001, 3759-3769; b) Y.-P. Sun, J. E. Riggs, B. Liu, *Chem. Mater.* 1997, **9**, 1268-1272; c) M. Cha, N. S. Sariciftci, A. J. Heeger, J. C. Hummelen, F. Wudl, *Appl. Phys. Lett.* 1995, **67**, 3850-3852.
- 4 a) L. Vivien, D. Riehl, J.-F. Delouis, J. A. Delaire, F. Hache, E. Anglaret, *J. Opt. Soc. Am. B* 2002, **19**, 208-214; b) K. Mansour, M. J. Soileau, E. W. Van Stryland, *J. Opt. Soc. Am. B* 1992, **9**, 1100-1109.
- 5 a) G. S. He, L.-S. Tan, Q. Zheng, P. N. Prasad, *Chem. Rev.* 2008, **108**, 1245-1330; b) H. M. Kim, B. R. Cho, *Chem. Commun.*, 2009, 153-164; c) C. Andraud, R. Fortrie, C. Barsu, O. Stéphan, H. Chermette, P. L. Baldeck *Photoresponsive Polymers II Book Series: Advances in Polymer Sciences* 2008, **214**, 149-203.
- 6 a) M. G. Silly, L. Porrès, O. Mongin, P.-A. Chollet, M. Blanchard-Desce *Chem. Phys. Lett.* 2003, **379**, 74-80; b) R. Anemian, Y. Morel, P. L. Baldeck, B. Paci, K. Kretsch, J.-M. Nunzi, C. Andraud, *J. Mater. Chem.* 2003, **13**, 2157-2163.
- 7 a) G.-J. Zhou, W.-Y. Wong, *Chem. Soc. Rev.*, 2011, **40**, 2541-2566; b) R. Westlund, E. Glimsdal, M. Lindgren, R. Vestberg, C. Hawker, C. Lopes, E. Malmstrom, *J. Mater. Chem.* 2008, **18**, 166-175; c) C. Girardot, B. Cao, J.-C. Mulatier, P. L. Baldeck, J. Chauvin, D. Riehl, J. A. Delaire, C. Andraud, G. Lemerrier *ChemPhysChem* 2008, **9**, 1531-1535.
- 8 a) K. S. Kim, S. B. Noh, T. Katsuda, S. Ito, A. Osuka, D. Kim, *Chem. Commun.* 2007, 2479-2481; b) S. A. Odom, S. Webster, L. A. Padilha, D. Peceli, H. Hu, G. Nootz, S.-J. Chung, S.

Ohira, J. D. Matichak, O. V. Przhonska, A. D. Kachkovski, S. Barlow, J.-L. Bredas, H. L. Anderson, D. J. Hagan, E. W. Van Stryland, S. R. Marder, *J. Am. Chem. Soc.* 2009, **131**, 7510-7511; c) S. Webster, S. A. Odom, L. A. Padilha, O. V. Przhonska, D. Peceli, H. Hu, G. Nootz, A. D. Kachkovski, J. Matichak, S. Barlow, H. L. Anderson, S. R. Marder, D. J. Hagan, E. W. Van Stryland, *J. Phys. Chem. B* 2009, **113**, 14854-14867; d) K. J. Thorley, J. M. Hales, H. L. Anderson, J. W. Perry, *Angew. Chem. Int. Ed.* 2008, **47**, 7095-7098. e) M. Drobizhev, Y. Stepanenko, A. Rebane, C. J. Wilson, T. E. O. Screen, H. L. Anderson *J. Am. Chem. Soc.* 2006, **128**, 12432-12433. f) K. Kamada, K. Ohta, T. Kubo, A. Shimizu, Y. Morita, K. Nakasuji, R. Kishi, S. Ohta, S.-I. Furukawa, H. Takahashi, M. Nakano, *Angew. Chem. Int. Ed.*, 2007, **46**, 3544-3546. g) K. Kamada, K. Ohta, A. Shimizu, T. Kubo, R. Kishi, H. Takahashi, E. Botek, B. Champagne, M. Nakano, *J. Phys. Chem. Lett.*, 2010, **1**, 937-940 ; h) S. Ellinger, K. R. Graham, P. Shi, R.T. Farley, T.T. Steckler, R. N. Brookins, P. Taranekar, J. Mei, L. A. Padilha, T. R. Ensley, H. Hu, S. Webster, D. J. Hagan, E. W. Van Stryland, K. S. Schanze, J. R. Reynolds, *Chem. Mater.* 2011, **23**, 3805-3817.

9 a) P.-A. Bouit, G. Wetzels, G. Berginc, B. Loiseaux, L. Toupet, P. Feneyrou, Y. Bretonniere, K. Kamada, O. Maury, C. Andraud, *Chem. Mater.* 2007, **19**, 5325-5335; b) P.-A. Bouit, R. Westlund, P. Feneyrou, O. Maury, M. Malkoch, E. Malmstrom, C. Andraud, *New J. Chem.* 2009, **33**, 964-968.

10 P.-A. Bouit, K. Kamada, P. Feneyrou, G. Berginc, L. Toupet, O. Maury, C. Andraud, *Adv. Mater.* 2009, **21**, 1151-1154.

11 Q. Zheng, G. S. He, P. N. Prasad, *Chem. Phys. Lett.* 2009, **475**, 250-255.

12 J. M. Hales, M. Cozzuol, T. E. O. Screen, H. L. Anderson, J. W. Perry, *Opt. Express* 2009, **17**, 18478-18488.

13 a) P.-A. Bouit, E. Di Piazza, S. Rigaut, B. Le Guennic, C. Aronica, L. Toupet, C. Andraud, O. Maury *Org. Lett.* 2008, **10**, 4159-4162; b) P.-A. Bouit, D. Rauh, S. Neugebauer, J. L.

Delgada, E. Di Piazza, S. Rigaut, O. Maury, C. Andraud, V. Dyakonov, N. Martin *Org. Lett.* 2009, **11**, 4806-4809; c) C. R. Nieto, J. Guilleme, C. Villegas, J. L. Delgado, D. Gonzalez-Rodriguez, N. Martin, T. Torres, D. M. Guldi *J. Mater. Chem.* 2011, **21**, 15914; L.A. Padilha, S. Webster, O.V. Przhonska, H. Hu, D. Peceli, T. R. Ensley, M. V. Bondar, A. O. Gerasov, Y.P. Kovtun, M. P. Shandura, A. D. Kachkovski, D. J. Hagan, E. Van Stryland *J. Phys. Chem. A.* 2010, **114**, 6493-6501.

14 P.-A. Bouit, C. Aronica, L. Toupet, B. Le Guennic, C. Andraud, O. Maury *J. Am. Chem. Soc.* 2010, **132**, 4328-4335.

15 S. Rigaut, C. Olivier, K. Costuas, S. Choua, O. Fadhel, J. Massue, P. Turek, J.-Y. Saillard, P. H. Dixneuf, D. Touchar *J. Am. Chem. Soc.* 2006, **128**, 5859-5876.

16 K. J. Thorley, J. M. Hales, H. L. Anderson and J. W. Perry, *Angew. Chem. Int. Ed.* 2008, **47**, 7095-7098.

17 K. Kamada, K. Matsunaga, A. Yoshino, K. Ohta, *J. Opt. Soc. Am. B* 2003, **20**, 529-537.

18 F. Terenziani, O. V. Przhonska, S. Webser, L. A. Padilha, Y. L. Slominsky, I. G. Davydenko, A. O. Gerasov, Y. P. Kovtun, M. P. Shandura, A. D. Kachkovski, D. J. Hagan, E. W. Van Stryland, A. Painelli *J. Phys. Chem. Lett.* 2010, **1**, 1800-1804.

19 a) S. Webster, J. Fu, L. A. Padilha, O. V. Przhonska, D. J. Hagan, E. W. Van Stryland, M. V. Bondar, Y. L. Slominsky, A. D. Kachkovski *Chem. Phys.* 2008, **348**, 143-151; b) J. Fu, L. A. Padilha, D. J. Hagan, E. W. Van Stryland, O. V. Przhonska, M. V. Bondar, Y. L. Slominsky, A. D. Kachkovski, *J. Opt. Soc. Am. B* 2007, **24**, 56-66; c) L. A. Padilha, S. Webster, O. V. Przhonska, H. Hu, D. Peceli, T. R. Ensley, M. V. Bondar, A. O. Gerasov, Y. P. Kovtun, M. P. Shandura, A. D. Kachkovski, D. J. Hagan, E. W. Van Stryland *J. Phys. Chem. A* 2010, **114**, 6493-6501.

20 a) L. Beverina, J. Fu, A. Leclercq, E. Zojer, P. Pacher, S. Barlow, E. W. Van Stryland, D. J. Hagan, J.-L. Brédas, S. R. Marder, *J. Am. Chem. Soc.* 2005, **127**, 7282-7283; b) S. Zheng, A.

Leclercq, J. Fu, L. Beverina, L. A. Padilha, E. Zojer, K. Schmidt, S. Barlow, J. Luo, S.-H. Jiang, A. K. Y. Jen, Y. Yi, Z. Shuai, E. W. Van Stryland, D. J. Hagan, J.-L. Brédas, S. R. Marder, *Chem. Mater.* 2007, **19**, 432-442.

21 a) S.-J. Chung, S. Zheng, T. Odani, L. Beverina, J. Fu, L. A. Padilha, A. Biesso, J. M. Hales, X. Zhan, K. Schmidt, A. Ye, E. Zojer, S. Barlow, D. J. Hagan, E. W. Van Stryland, Y. Yi, Z. Shuai, G. A. Pagani, J.-L. Brédas, J. W. Perry, S. R. Marder, *J. Am. Chem. Soc.* 2006, **128**, 14444-14445; b) K. Kurotobi, K. S. Kim, S. B. Noh, D. Kim, A. Osuka, *Angew. Chem. Int. Ed.* 2006, **45**, 3944-3947; c) T. K. Ahn, K. S. Kim, D. Y. Kim, S. B. Noh, N. Aratani, C. Ikeda, A. Osuka, D. Kim *J. Am. Chem. Soc.* 2006, **128**, 1700-1704. d) M.-C. Yoon, S. B. Noh, A. Tsuda, Y. Nakamura, A. Osuka, D. Kim *J. Am. Chem. Soc.* 2007, **129**, 10080-10081.

22 M. Sheik-Bahae, A. A. Said, T.-H. Wei, D. J. Hagan, E. W. Van Stryland *IEEE J. Quant. Electron.*, 1990, **26**, 760-769.

23 D. I. Kovsh, S. Yang, D. J. Hagan, E. W. Van Stryland *Appl. Opt.*, 1999, **38**, 5168-5180.

TOC

Excited state absorption: a key phenomenon for the generation of an efficient biphotonic based optical limiting behavior at telecommunication wavelengths.

Quentin Bellier, Nikolay S. Makarov, Pierre-Antoine Bouit, Stéphane Rigaut, Kenji Kamada, Patrick Feneyrou, Gérard Berginc, Olivier Maury*, Joseph W. Perry*, and Chantal Andraud*.

Cyanine ns-Optical Power Limiting

